

BEHAVIOR OF SC WALL LAP-SPLICE ANCHORAGES

Amit H. Varma¹, Jungil Seo², Hoseok Chi³, Tod Baker⁴

¹Assoc. Prof., Bowen Lab., School of Civil Eng., Purdue Univ., W. Lafayette, IN. ahvarma@purdue.edu

²Ph.d Candidate, Bowen Lab., School of Civil Eng., Purdue Univ., W. Lafayette, IN. seo2@purdue.edu

³Research Scientist, Bowen Lab., School of Civil Eng., Purdue Univ., W. Lafayette, IN.

⁴Fellow Eng., Westinghouse Elec. Corp., Cranberry Township, PA. bakerth@westinghouse.com

E-mail of corresponding author: ahvarma@purdue.edu

ABSTRACT

Steel-plate composite (SC) walls can be anchored to reinforced concrete (RC) foundations using lap splice anchorages. Researchers in Japan have conducted extensive large-scale tests to evaluate the strength and ductility of these lap splice anchorages for the critical loading of cyclic axial tension. The parameters included were the tie bar reinforcement ratio, the clear distance from the dowel bars to the steel plates, and the embedment length. The experimental results are presented in this paper in detail, and analytical models are benchmarked to predict their behavior. Additional large-scale tests are conducted to further demonstrate the strength and ductility of lap-splice anchorages with adequate tie bar ratios and embedment length but significant eccentricity (distance between dowel bars and steel plates). The benchmarked models are used to gain additional insight into the behavior and force transfer in the lap-splice anchorage. The results from all the experimental and analytical investigations are used to provide design and detailing recommendations for lap-splice anchorages and to obtain ductile behavior.

INTRODUCTION

Modularization with steel-plate composite (SC) walls has been proposed and studied to reduce the construction period and cost for safety related nuclear facilities [1]. SC walls consist of steel faceplates (0.25 to 1.5 in. thick) that are connected to each other and the concrete infill (18 – 60 in. thick) with steel headed stud anchors (studs), and steel tie bars. These SC walls are different from RC walls in that there are no steel rebars that can be continued or developed into the foundation for anchorage. SC walls can be anchored into the RC foundation using different techniques. For example, (i) the steel plates can be continued and embedded into the concrete foundation using shear connectors and rebars welded to the steel plates, or (ii) the steel plates can be welded to baseplates with anchor bars that are embedded into the concrete foundation, or (iii) steel dowel bars can be used transfer the forces from the SC wall to the RC foundation.

Connection type (iii) is referred as a lap-splice anchorage because the dowel bars are lap spliced with the steel faceplates of the SC walls. The dowel bars can be anchored into the RC foundation using their ACI 349 calculated development length [2]. However, this type of lap-splice anchorage raises some questions about the lap length in the SC portion of the structure, the design of the shear connectors (studs) to transfer forces between the steel faceplates to the rebar dowels, and the design of tie bars to facilitate force transfer while maintaining structural integrity (preventing splitting failure) of the SC composite system. The design philosophy for this type of anchorage connection is to develop either yielding of the steel faceplates of the SC walls, or yielding of the steel dowel bars in tension. Both of these are ductile yielding limit states that will enable the lap splice anchorage to demonstrate ductility and energy dissipation during earthquake loading. Non-ductile limit states like pullout of the dowel bar, splitting failure of the SC wall section, failure of studs etc. have to be prevented.

Katayama et al. [3] conducted full scale tests to evaluate the strength and ductility of this type of SC to RC lap splice anchorage region. They tested nine (a-i) SC to RC lap splice anchorage specimens with different parameters such as number of dowel bars, location of dowel bars, development length, tie bar area, and dowel bar size. This paper presents the experimental behavior and results, and the development and benchmarking of 3D finite element models for predicting the behavior of these anchorage specimens.

Additionally, the authors designed and tested two lap-splice anchorage specimens to evaluate their design strength and ductility, which are included in the paper along with their benchmarked analytical (finite element) models and results. The results from all the experimental and analytical studies are used to provide design and detailing recommendations for these lap-splice anchorages.

EXPERIMENTAL EVALUATIONS BY KATAYAMA et al. [3]

Katayama et al. [3] conducted nine full-scale tests to investigate the behavior of SC wall-to-RC foundation lap splice anchorages. Figure 1 shows the typical configuration of the test specimens. As shown, the specimens included the SC wall portion of the anchorage only. The concrete portion of the RC foundation was not included because it is not expected to have an influence on the axial tension behavior of the anchorage joint. Steel dowel bars were embedded into the SC walls, and they extended out of the concrete. Axial tension was applied by pulling the dowel bars using a specially designed setup.

The specimen details are given in Table 1, which includes the width and thickness of the steel plates, the depth of the composite section, the dowel bar diameter, and the length of dowel embedment into the SC wall as function of the dowel diameter (d_b). The Table also includes the concrete measured compressive and tensile strengths, and the measured yield strengths of the steel faceplates, dowel bars, studs, and tie bars. In Table 1, the term α represents the distance from the dowel bar to the steel faceplate divided by the dowel bar diameter (d_b). The tie bar ratio is calculated as the area of the tie bar divided by the tributary area of concrete associated with it.

As shown in Table 1, most of the specimens had a dowel embedment length of 40 times the dowel bar diameter (d_b) with the exception of Specimen e, which had an embedment length of 50 d_b . These dowel embedment lengths are comparable to the ACI [2] calculated development lengths for Grade 60 rebars in 4000 psi concrete, which are about 47 times d_b .

Most of the specimens were 35.4 in. deep with the exception of Specimen f, which was 47.2 in. deep. Most of the specimens had 1.5 in. diameter dowel bars, with the exception of Specimens b and f, which had 2 in. diameter dowel bars. The parameter α varied significantly between the specimens, and so did the tie bar ratio. Specimen h had no tie bars, and Specimen g had very low tie bar ratio. Specimens a and b had the highest tie bar ratios.

The concrete compressive strengths were approximately 5000 psi (4779-5277 psi). The steel faceplate yield strengths were slightly larger than 50 ksi (50.7 – 58.6 ksi). The dowel bar yield strengths were very high (greater than 100 ksi in most cases). All the specimens were designed such that the steel faceplate yielding would occur significantly before dowel bar yielding. The studs and tie bars had yield strengths of approximately 41 ksi and 48 ksi, respectively. The shear studs were 0.625 in. in diameter, and had spacing of 7.9 in. The tie bar diameters varied from 0.625 – 0.875 in. They were welded to the steel faceplates, and had longitudinal and transverse spacing of 7.9 – 9.9 in.

The cyclic loading protocol consisted of half cycles of tension loading as follows. Three half cycles each at 30%, 50%, 70%, 90% and 100% of the yield strength of the dowel bars. Three half cycles at 100% of the yield strength of the steel plates, and three half cycles at 2 and 5 times the yield displacement (δ_y), where δ_y is the displacement corresponding to yielding of the steel plates.

The experimental results are presented in Figures 2-5, wherein the term displacement is the longitudinal displacement due to strain of faceplates and dowel bars, slippage between faceplates and concrete infill, and pullout of dowel bars from concrete infill. Two failure modes were observed: (i) yielding of the steel faceplates and dowels, and (ii) pullout or bond failure.

As shown in Figures 2-5, Specimens a and b with the largest tie bar ratios and reasonable α factors (of 4.1) developed yielding of the steel faceplates and dowel bars. Specimens c and e with low tie bar ratios had ductile behavior under the applied loading, but eventually suffered bond failure after extensive yielding and displacement of the steel plates. All the remaining specimens (d, f, g, h, and i) had bond or pullout failure with little to no yielding of the steel faceplates.

Figures 2 and 3 demonstrate the effects of tie bar reinforcement ratio (ρ_w) on the behavior of lap-splice anchorage specimens. As shown, reducing the tie bar reinforcement ratio, while maintaining the α parameter at 4.1, reduces the load carrying capacity and ductility of the anchorage connection. The failure mode also changes from yielding of steel faceplates and dowels to bond or pullout failure.

Figure 4 demonstrates the effects of α parameter (distance from steel plate to dowel bar) on the behavior of lap-splice anchorage specimens with low tie bar reinforcement ratios of 0.17%. As shown, increasing the α parameter (from 1.0 to 4.1 to 5.5) reduces the load carrying capacity and ductility of the anchorage connection with low reinforcement ratio. This occurs because increasing the α factor increases the connection eccentricity, and causes greater tendency for splitting failure of the composite section, which can be resisted by the tie bars (if adequately present).

Figure 5 demonstrates the effects of increasing the embedment length on the behavior of specimens with low tie bar ratio (0.17%) and reasonable α factor (4.1). As shown, increasing the embedment length can improve the lap-splice anchorage strength and ductility, but bond failure may still occur in the absence of adequate tie bar ratio.

Table 1: Summary of test specimens

Specimen	Width (in.)	Depth (in.)	Plate thick. (in.)	Dowel dia. d_b (in.)	Embedded length	Concrete Strength		Steel Strength				α	Tie bar ratio (%)
						Comp. (psi)	Ten. (psi)	Plate (ksi)	Dowel (ksi)	Stud (ksi)	Tie (ksi)		
a	31.5	35.4	0.24	1.50	40 d_b	5277	354.2	58.6	105.6	41.4	48.0	4.1	0.50
b	29.5	47.2	0.35	2.01	40 d_b	5106	415.3	50.7	99.3	44.3	46.7	3.5	0.61
c	31.5	35.4	0.24	1.50	40 d_b	5234	384.0	55.4	105.6	41.4	48.7	1.0	0.17
d	31.5	35.4	0.24	1.50	40 d_b	5092	355.6	57.4	105.6	41.4	48.7	5.5	0.17
e	31.5	35.4	0.24	1.50	50 d_b	4779	384.0	57.1	105.6	41.4	48.7	4.1	0.17
f	29.5	47.2	0.35	2.01	40 d_b	5234	386.9	53.3	99.3	44.3	46.7	3.5	0.30
g	31.5	35.4	0.24	1.50	40 d_b	4921	411.1	58.1	105.6	41.4	48.7	4.1	0.11
h	31.5	35.4	0.24	1.50	40 d_b	5163	347.1	56.6	105.6	41.4	-	1.0	0.00
i	31.5	35.4	0.24	1.50	40 d_b	4850	406.8	56.0	77.1	47.0	46.8	4.1	0.17

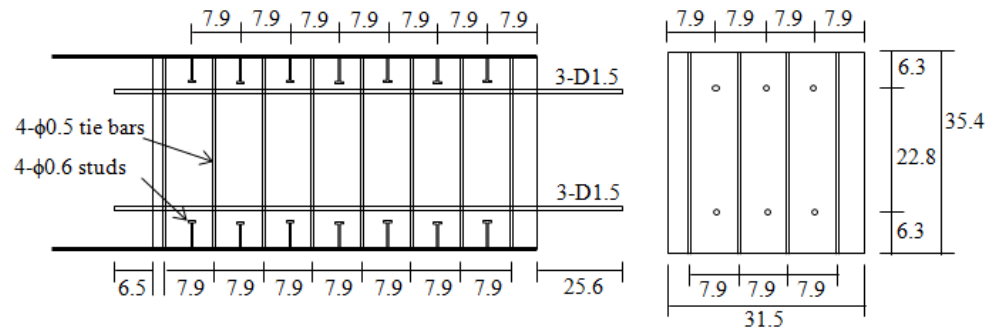


Fig. 1: Typical configuration of test specimens (dimensions in in.)

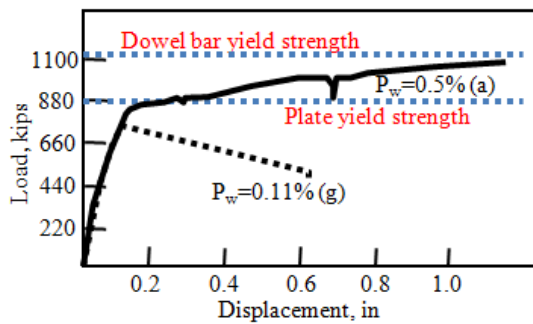


Fig. 2: Load versus displacement curves with the effect of tie bar area (1.5 in. dowel bar size)

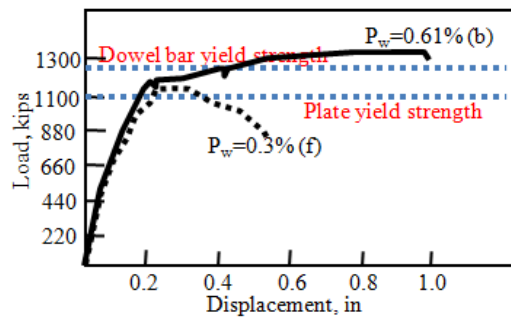


Fig. 3: Load versus displacement curves with the effect of tie bar area (2 in. dowel bar dia)

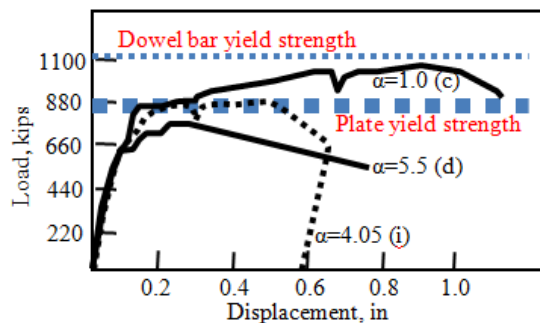


Fig. 4: Load versus displacement curves with the effect of dowel bar location

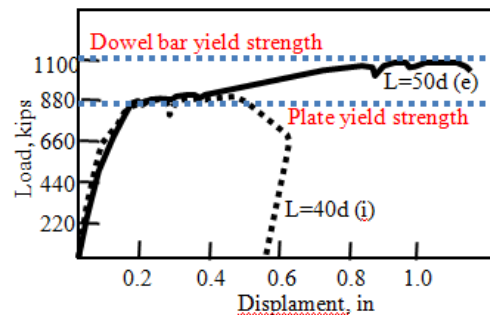


Fig. 5: Load versus displacement curves with the effect of embedded dowel bar length

BENCHMARKING ANALYSIS FOR KATAYAMA et al. [3] EXPERIMENTS

A detailed 3D finite element model was developed using ABAQUS for the SC-RC lap splice connection specimens tested by Katayama et al. [3]. The steel plates, shear studs, and tie bars were modeled in 3D using C3D8R (eight-node solid elements with reduced integration) elements. The concrete infill was also modeled using C3D8R elements.

The contact interaction between the steel plate and the concrete infill was assumed as follows: (i) in the normal direction, hard contact was assumed. (ii) In the tangential direction, the coefficient of friction was assumed to be equal to 0.6. The finite elements modeling the studs and the tie bars were fully embedded in the concrete finite elements.

The mesh size for the tie bars was 1 in., and the mesh size for the concrete elements was 1 in. The same steel material properties were assumed. However, uniaxial tension stress-strain curves were generated using the measured material properties.

The concrete was modeled using the concrete damaged plasticity model in ABAQUS. The Popovics [4] model was used to develop the uniaxial compression stress-strain curve, and the Wittman [5] tension cracking model was used to develop the tension stress-crack opening displacement curve for concrete. These compression and tension stress behavior models are shown in Figures 7 and 8, respectively.

Monotonic displacement of 1 in. was applied at the ends of the dowel bars, while restraining the steel plate ends similar to the test specimens. All the 3D finite element models were analyzed for pseudo-static loads using explicit dynamic analysis procedures with semi-automatic mass scaling. The kinetic and strain energies in the models was tracked through out the analyses, and the results were discarded in case of anomalies, i.e., the kinetic energy exceeds the strain energy by 5% or more.

Figures 8-13 compare the analytically predicted load-displacement curves with those measured experimentally by Katayama et al. [3] for Specimens a-f. As shown, the experimental and analytical curves compare very well for Specimens a and b, which had ductile yielding of the steel plates and dowel bars and no bond or pullout failure due to adequate tie bar ratios. The comparisons for specimens c-f shown in Figures 10-13 are reasonable in the ductile range of the behavior, but as expected the finite element models could not predict (with confidence) the final brittle failure modes such as shear bond, bond splitting, or pullout failure of the dowel bars.

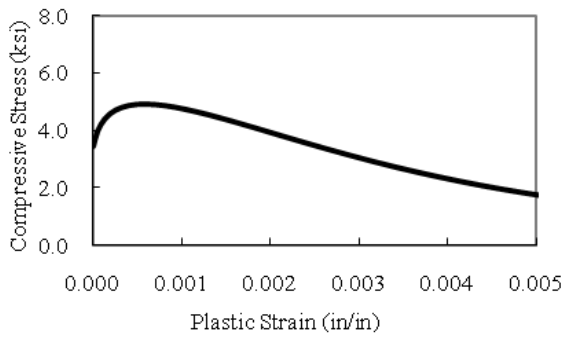


Fig. 6: Compressive stress versus plastic strain curve for concrete infill

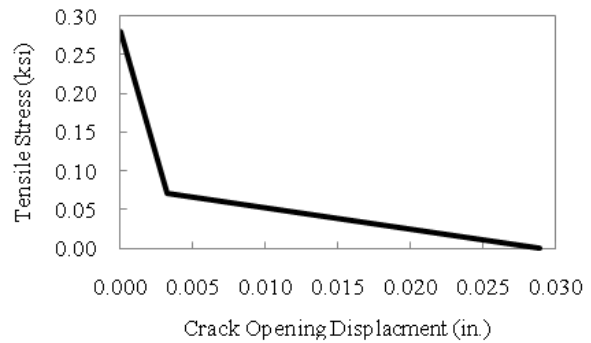


Fig. 7: Tension softening curve for concrete infill

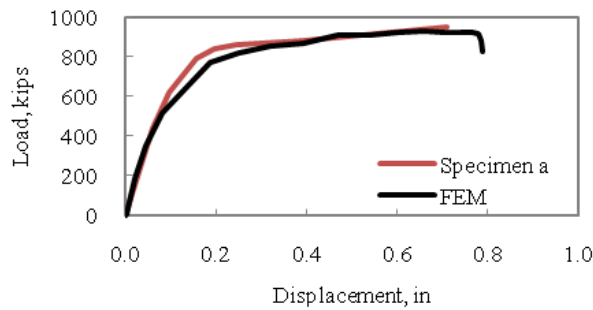


Fig. 8: Comparison of load versus displacement curves for Specimen a

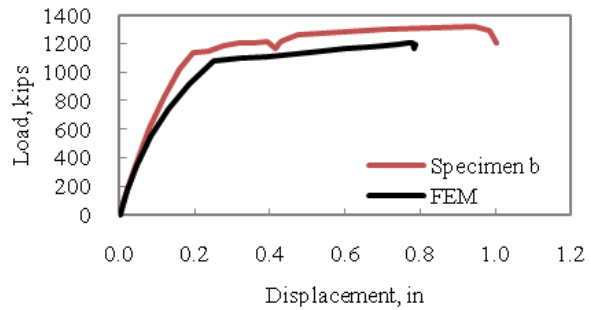


Fig. 9: Comparison of load versus displacement curves for Specimen b

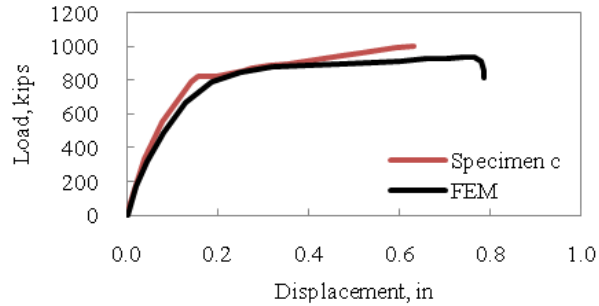


Fig. 10: Comparison of load versus displacement curves for Specimen c

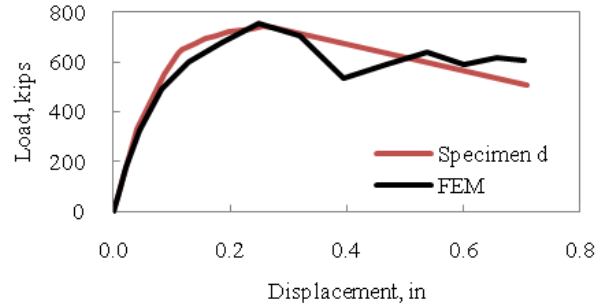


Fig. 11: Comparison of load versus displacement curves for Specimen d

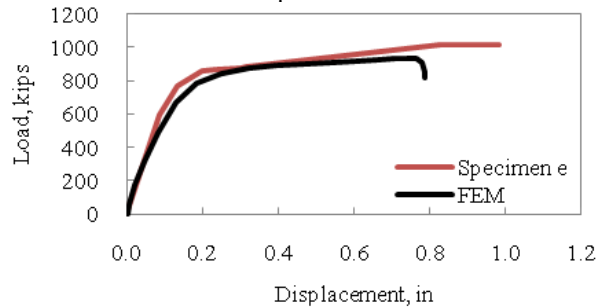


Fig. 12: Comparison of load versus displacement curves for Specimen e

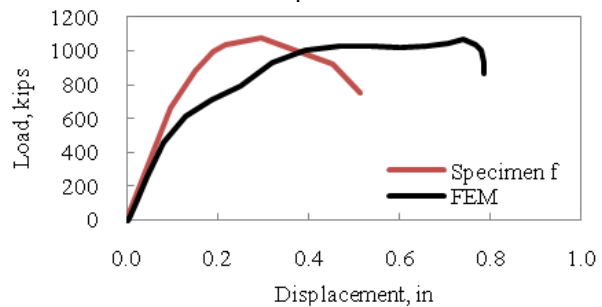


Fig. 13: Comparison of load versus displacement curves for Specimen f

ADDITIONAL LAP-SPLICE ANCHORAGE TESTS

The authors have further conducted full-scale SC-to-RC lap-splice anchorage connection tests to evaluate their strength and ductility in the presence of significant eccentricity, i.e., dowel bars located much further away from the steel plates. The SC-RC lap splice anchorage specimens consisted of steel faceplates, tie bars, concrete infill, and #11 dowel bars. Figures 14 and 15 show an elevation view of the test specimen (without the concrete infill) and the layout of #11 dowel bars, respectively.

As shown, the width of the steel faceplates was 0.63 times of the depth of the specimen (T) and the thickness was 0.02 T . These faceplates were anchored to the concrete infill using tie bars that were welded to the steel faceplates and had a longitudinal spacing of 0.16 T , and transverse spacing of 0.12 T , resulting in a tie bar ratio of more than 1%. The concrete infill had nominal compressive strength equal to 6 ksi.

The test specimens had sixteen #11 (1.375 in.) steel dowel bars. These dowel bars were located in four layers of four dowel bars each. Two layers of #11 dowel bars were close to each steel faceplate of the SC portion. The first layer was located at a spacing of $5.31d_b$ from the steel faceplate, and the second layer was located at a spacing of $8.87d_b$ from the steel faceplate. The transverse spacing of the #11 dowel bars is equal to $3.2d_b$.

The uniaxial tension was applied to the steel faceplates of the SC region and the dowel bars of the RC region using the test setup shown in Figure 16. The tension loading was applied using two 1000-kip capacity hydraulic rams. The steel faceplates were bolted to loading beam 1, and the #11 dowel bars were attached to loading beam 2 using certified mechanical couplers and threaded rods. The applied tension was transferred from the steel faceplates to the dowel bars through the SC-to-RC connection region.

Figure 17 shows the measured load versus displacement of the test specimen, where the axial displacement was measured from the top steel plate to the loading beam 2. The maximum applied load was about 2021 kip, which is much greater the measured yield strength of the steel faceplates or the sixteen #11dowel bars. The load-displacement behavior was governed completely by ductile yielding of the steel faceplates and the dowel bars. There was no brittle failure even at the end of the test. This demonstrates the excellent behavior of lap-splice anchorage specimens with adequate tie bar ratio ($>1\%$), which is ductile and governed by yielding of the steel elements.

Figure 18 shows the applied load vs. average longitudinal strain in one of the #11 dowel bars. The longitudinal strain was determined by averaging the measurement of four strain gages around the circumference of the dowel bar. Similarly, Figures 19 and 20 show the applied load vs. average longitudinal strain in the top and bottom steel plates of the SC portion just at the end of the connection region. As shown in Figures 18-20, the dowel

bars and steel plates underwent significant yielding and ductile behavior during the test (20,000 microstrain was the maximum strain that could be measured by the strain gages used).

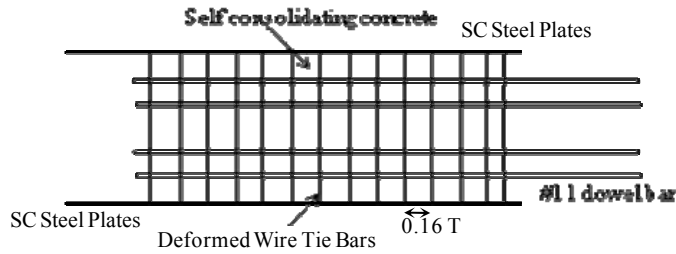


Fig. 14: Elevation view of test specimen

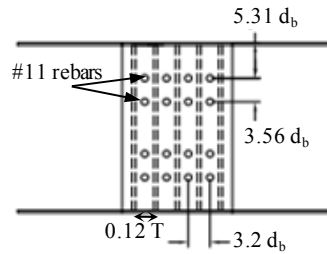


Fig. 15: #11 dowel bar layout

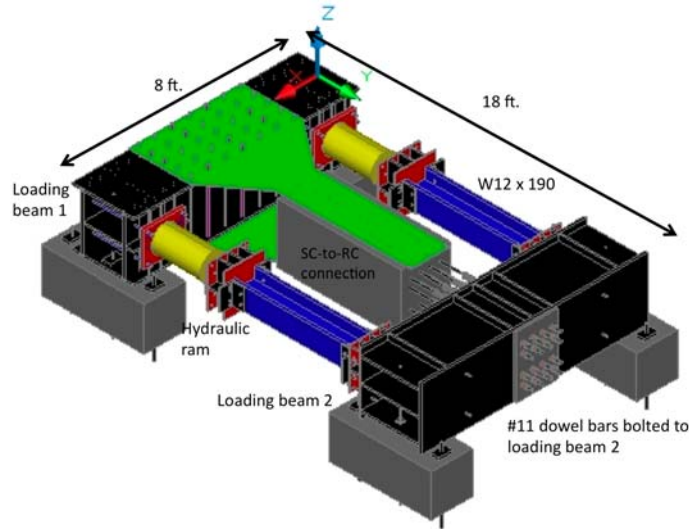


Fig. 16: Test Setup for SC-to-RC Connection Region Test

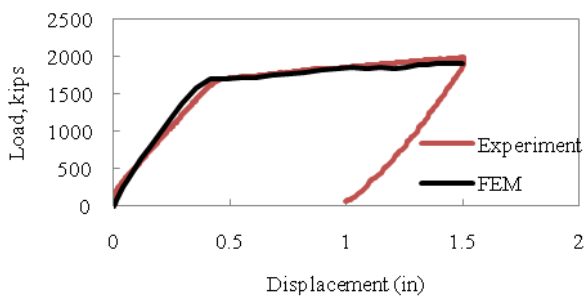


Fig. 17: Load versus displacement curve

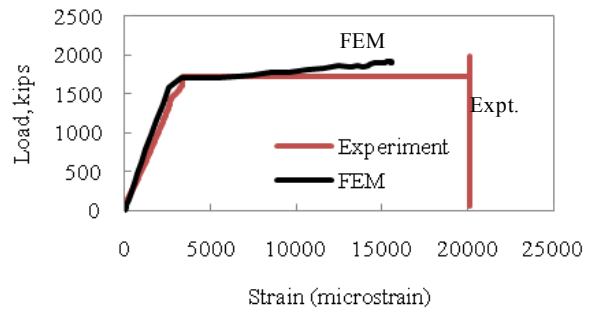


Fig. 18: Averaged longitudinal dowel bar strain

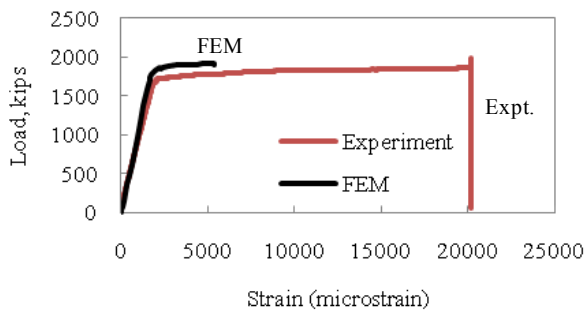


Fig. 19: Load versus longitudinal strains in top plate

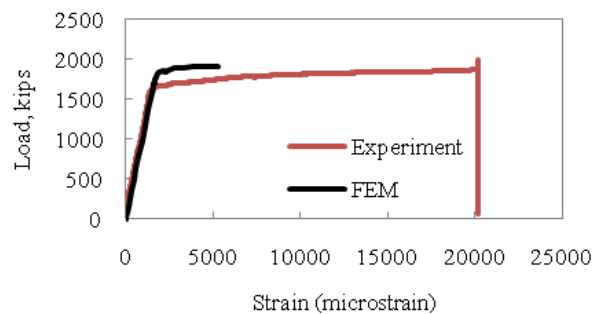


Fig. 20: Load versus longitudinal strains in bottom plate

ANALYTICAL INSIGHT INTO BEHAVIOR

The 3D finite element models developed for Katayama et al.’s [3] test specimens were used to predict the behavior of the SC-to-RC lap-splice anchorage specimen tested by the authors. It included the meshes for the steel plates, tie bars, and the concrete infill, and was identical (in all material and modeling details) to the finite element models described earlier for Katayama’s specimens.

Figures 21-25 show the finite element model stress and strain states at 2040 kips, which corresponds to the peak load. Figure 21 shows Von Mises stress contours for the steel plates, and illustrates extensive yielding (grey region above 55 ksi stress) of the steel plates outside the connection (force transfer) region. Figure 22 shows the Von Mises stress contours for the dowel bars, and illustrates extensive yielding (grey region above 73 ksi stress) along the length of the #11 dowel bars.

Figures 23-25 focus on the concrete stress and strain states at 2040 kips applied loading. Figure 23 shows the plastic tensile strain in the concrete, where values greater than 0.003 indicating visible cracking are shown in grey contours. Figure 24 shows the direction vector for the maximum principal strain (causing cracking perpendicular to it) in the concrete. Figure 25 shows contour plots of the minimum principal stress (compression struts) in the concrete. These Figures show the extent of cracking in the concrete and the formation of compression struts to transfer the axial tension from the steel plates to the #11 dowel bars clearly. Figure 26 shows a photograph of the observed concrete crack map in the specimen after testing. As shown, the cracking in Figure 26 compares very well with the concrete state in Fig. 23-25

Figure 17 includes comparison of the analytically predicted and experimentally measured applied load-displacement curves. Similarly, Figures 18, 19, and 20 include comparisons of the analytically predicted and experimentally measured applied load – average longitudinal strain curves for the #11 dowel bars, top steel plate, and bottom steel plate, respectively. As shown, the analytical prediction compare very well with the experimental results. These comparisons are excellent at the global level (Figure 27), and also at the local level (Figures 28-30) where yielding of the steel plates and dowel bars occurs.

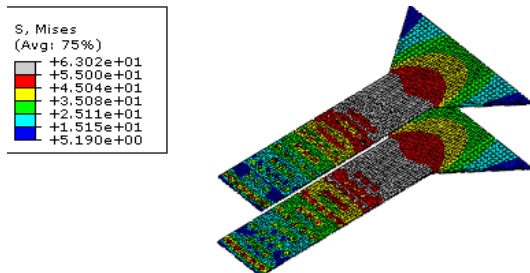


Fig. 21: Von Mises stress in steel plates at 2040 kips

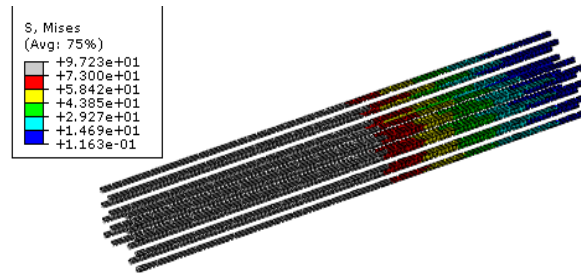


Fig. 22: Von Mises stress in dowel bars at 2040 kips

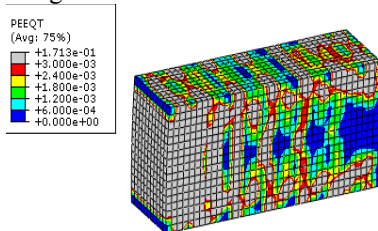


Fig. 23: Plastic strain in tension at 2040 kips

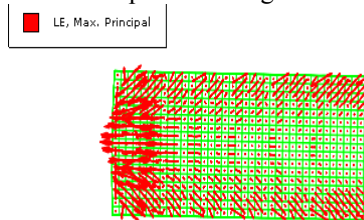


Fig. 24: Vector plot of maximum principal strain at 2040 kips

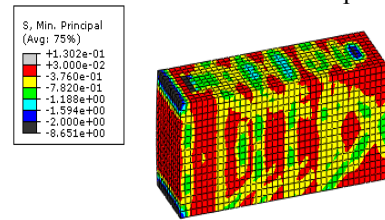


Fig. 25: Minimum principal stress at 2040 kips



Fig. 26: Concrete crack map after test completion

CONCLUSIONS AND DESIGN RECOMMENDATIONS

This paper presented the results from large-scale experimental and analytical investigations of the axial tension behavior of SC wall -to-RC foundation lap-splice anchorages. The experimental investigations included the parameters: tie bar ratio (ρ_w), distance between SC wall and dowel bar (α), and dowel embedment length. The experimental and analytical results indicate that:

1. The axial load-displacement behavior of SC-to-RC lap splice anchorages can be governed by the ductile yielding of the steel plates and steel dowel bars, or the non-ductile bond splitting or pullout failure of dowel bars
2. Specimens with adequate embedment length ($\geq 40 d_b$) and tie bar ratio ($\geq 0.5\%$) have excellent ductility with yielding of the steel faceplates and steel dowel bars governing the axial load – displacement behavior.
3. If the tie bar ratio is low or inadequate ($< 0.3\%$), then increasing the parameter α can reduce the strength and ductility of the connection. However, such designs are not recommended.
4. Increasing the embedment length can generally improve the strength and ductility of the connection, however, this works better for designs with adequate tie bar ratio ($>0.5\%$).
5. 3D finite element models can be developed and used to predict the behavior of SC wall-to-RC foundation lap splice anchorages governed by ductile yielding of steel plates or dowel bars with reasonable confidence. These models do not necessarily predict the non-ductile failure modes accurately.

SC wall-to-RC foundation lap-splice anchorages should be designed to have ductile behavior governed by the yielding of the steel plates and dowel bars. This can be accomplished by: (i) providing adequate number and spacing of shear connectors to transfer the forces from the steel plates to the dowel bars, (ii) having adequate development length in the SC portion (at least greater than or equal to 40 times the bar diameter), and (iii) having adequate tie bar reinforcement ratio of at least 0.5%. As shown by the author's tests, the dowel bars can be located much further away from the steel plates if adequate tie bar reinforcement ratio is provided.

ACKNOWLEDGMENTS

The research presented in this paper was partially funded by Westinghouse Electric Corp. All findings presented in the paper are strictly those of the authors.

REFERENCES

- [1] JEAG 4618, "Technical Guidelines for A Seismic Design of Steel Plate Reinforced Concrete Structures: Buildings and Structures", Japanese Electric Association Nuclear Standards committee, 2005.
<http://www.ne.doe.gov/np2010/reports/mpr2610Rev2Final1924.pdf>
- [2] MPR-2610 Revision 2, "Application of Advanced construction Technologies to New Nuclear Power Plants", Department of Energy Report, September 2004,
- [3] Katayama et al., "Experimental study on a concrete filled steel structure", *Summaries of Technical Papers of Annual Meeting*, Architectural Institute of Japan, Vol. 33 and 34, 1999.
- [4] Popovics, S., *Mechanical Behavior of Materials, Proceedings of the International Conference on Mechanical Behavior of Materials*, The Society of Materials Science, Japan, Vol. IV, 1972, pp. 172-183.
- [5] Wittman, F.H. et al., "Fracture energy and strain softening of concrete as determined by means of compact tension specimens", *Materials and Structures/Materiaux et Constructions*, Vol. 21, 1988, pp. 21-32.
- [6] ACI 349-06. *Code Reqs. for Nuclear Safety Related Conc. Struct. and Comm.* ACI, Farmington Hills, MI.